Energy Model to Evaluate Thermal Energy Storage Integrated with Air Source Heat Pumps

Preprint

Conrado Ermel,[1] Marcus V.A. Bianchi,[1] and Paulo S. Schneider[2]

1 National Renewable Energy Laboratory
2 Federal University of Rio Grande do Sul

Presented at the 2022 Buildings XV International Conference
Clearwater Beach, Florida
December 5-8, 2022

NREL is a national laboratory of the U.S. Department of Energy
Office of Energy Efficiency & Renewable Energy
Operated by the Alliance for Sustainable Energy, LLC

This report is available at no cost from the National Renewable Energy Laboratory (NREL) at www.nrel.gov/publications.

Contract No. DE-AC36-08GO28308

Conference Paper
NREL/CP-5500-82601
January 2023

Energy Model to Evaluate Thermal Energy Storage Integrated with Air Source Heat Pumps

Preprint

Conrado Ermel,[1] Marcus V.A. Bianchi,[1] and Paulo S. Schneider[2]

1 National Renewable Energy Laboratory
2 Federal University of Rio Grande do Sul

Suggested Citation
Ermel, Conrado, Marcus V.A. Bianchi, and Paulo S. Schneider. 2023. *Energy Model to Evaluate Thermal Energy Storage Integrated with Air Source Heat Pumps: Preprint*. Golden, CO: National Renewable Energy Laboratory. NREL/CP-5500-82601. https://www.nrel.gov/docs/fy23osti/82601.pdf.

Conference Paper
NREL/CP-5500-82601
January 2023

National Renewable Energy Laboratory
15013 Denver West Parkway
Golden, CO 80401
303-275-3000 • www.nrel.gov

NOTICE

This work was authored in part by the National Renewable Energy Laboratory, operated by Alliance for Sustainable Energy, LLC, for the U.S. Department of Energy (DOE) under Contract No. DE-AC36-08GO28308. Funding provided by the U.S. Department of Energy Office of Energy Efficiency and Renewable Energy Buildings Technologies Office. The views expressed herein do not necessarily represent the views of the DOE or the U.S. Government. The U.S. Government retains and the publisher, by accepting the article for publication, acknowledges that the U.S. Government retains a nonexclusive, paid-up, irrevocable, worldwide license to publish or reproduce the published form of this work, or allow others to do so, for U.S. Government purposes.

Cover Photos by Dennis Schroeder: (clockwise, left to right) NREL 51934, NREL 45897, NREL 42160, NREL 45891, NREL 48097, NREL 46526.

Energy Model to Evaluate Thermal Energy Storage Integrated with Air Source Heat Pumps

Conrado Ermel
Ph.D. Candidate

Marcus V.A. Bianchi
ASHRAE Member

Paulo S. Schneider
Associate Professor

ABSTRACT

Full decarbonization in buildings requires the replacement of combustion appliances with electric ones, and air source heat pumps (ASHP) are a candidate alternative. However, technical limitations, such as the efficiency decrease when operating in cold weather, limit their adoption in the global heating market. Among several options to improve ASHP efficiency operating in colder climates, thermal energy storage (TES) has been considered, as it may provide heating when it is cold and shift ASHP operation to times when the weather is warmer. It may also take advantage of time of use electricity rates and support defrosting when necessary. The evaluation of ASHP-TES systems, however, is still limited because traditional metrics do not capture their full economic and environmental benefits. In this work, a python framework is presented to model the ASHP with and without the presence of TES. Metrics are proposed to analyze the system performance in terms of costs, equivalent CO_2 emission, and efficiency metrics to evaluate and compare alternative systems. Model validation against experimental data obtained for a commercial heat pump is provided, as well as an application example using Denver, Colorado, to highlight the model capabilities.

INTRODUCTION

Buildings represent about 12% of the end-use CO_2 emissions in the United States (IEA, 2022a), and 36% in the EU (Le et al., 2019), hence, reducing emissions is profoundly needed. Several strategies have been proposed in recent years to mitigate the climate crisis, one of which is electrification as a way of decarbonizing buildings (Carroll et al., 2020; Le et al., 2020). Numerous studies proposed replacing combustion appliances with electrical heat pumps (da Cunha and Eames, 2016; Hirvonen and Sirén, 2017; Le et al., 2020; Carroll et al., 2020; Vering et al., 2022), because when electricity generation has a high penetration of renewables, the electrification of heating systems may support the curb of carbon dioxide emission (Bianco et al., 2017). Beyond the environmental benefits, replacing combustion appliances with electric heat pumps can have a geopolitical benefit as well, since it can reduce the dependence on natural gas imports (IEA, 2022b).

Although they can be part of the electrification of buildings, air source heat pumps (ASHP) operating in very cold climates face technical and economic challenges, since their performance is compromised (Moreno et al., 2014). As it gets colder, the temperature difference between the conditioned space and the outdoor air is higher, forcing the ASHP to operate at a larger pressure difference between the condenser and the evaporator, thus reducing the coefficient of performance (COP) and the heating capacity, eventually leading to shut down (Long et al., 2014; Wang et al., 2017; Dincer et al., 2017). Also, depending on the outdoor conditions, ice can form on the evaporator (external unit), reducing even more the system performance, and requiring defrosting strategies, which further reduces the seasonal performance and deteriorates thermal comfort (Wang et al., 2017).

Thermal energy storage (TES) is a candidate to support heat pumps (HP) in cold climates. It has been integrated to HPs to prevent their operation when the outdoor temperature is very low or to shift the load to off-peak hours (da Cunha and Eames, 2016; Sevault et al., 2019; Li et al., 2020; Ermel et al., 2022a). It can supply the heating load allowing the HP to only operating when the utility rate and the external conditions are favorable. Operating the HP when it is not too cold increases its COP and the flexibility introduced by TES allows prioritizing the HP operation when the electricity rates are lower (da Cunha and Eames, 2016). TES was also employed to reduce the defrosting times (Jiankai et al., 2012) and

improve the thermal comfort (Long et al., 2014).

Some studies focused on evaluating the system performance for different regions. Yu et al. (2021) presented a techno-economic analysis of a latent TES integrated with an ASHP for space heating in China. A comparison between the ASHP-TES system with natural gas boilers and coal furnaces was presented, highlighting that the CO_2 emissions and the running costs are strictly dependent on (1) the energy mix to generate electricity, (2) the fuel costs, and (3) the climate. TES may also help HP water heater in Canada and the United States as demonstrated by (Treichel and Cruickshank, 2021).

In the present study we expanded a Python framework developed by the authors (Ermel et al., 2022b) to investigate the hourly performance of a space heating system composed of an ASHP integrated with a water tank (sensible TES) operating as a buffer between the HP and the conditioned space. A case study to illustrate the model capabilities with a combined system operating in Denver, CO was presented. There, a basic operation logic was proposed with the HP charging the TES when the outdoor temperature is relatively higher and the TES discharging it to the conditioned space when the outdoor temperature is low. The hybrid ASHP-TES solution was compared to a HP operating without TES to explore the differences in performance. In addition to the traditional metrics (COP and seasonal performance) we also analyzed the results for CO_2 emissions and running costs.

MATHEMATICAL MODEL

Heat Pump

We considered the space heating system shown in Figure 1a. A quasi-steady state physics-based model was developed to represent the vapor compression cycle and determine the states of points 1-4.

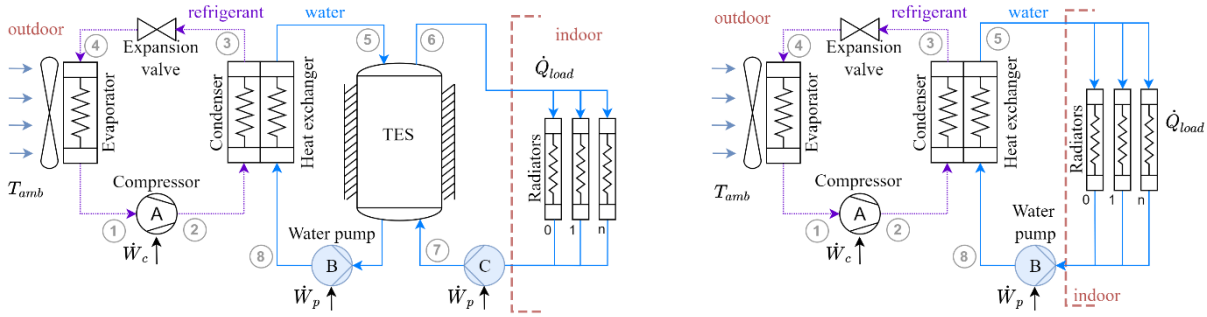

a b

Figure 1 Space heating system: (a) heat pump with TES, (b) heat pump without TES

An energy balance on the condenser allows to calculate the refrigerant states at points 2 and 3,

$$\dot{Q}_{cond} = \dot{m}_r(h_3 - h_2) = \varepsilon_{cond}\dot{m}_w Cp_w(T_2 - T_8), \quad (1)$$

where ε_c is the heat exchanger effectiveness, $\dot{m}_w$ is the water mass flow rate, Cp_w the specific heat of water, with the temperatures in points 2 and 8 denoted by T_2 and T_8, respectively. For the evaporator, the energy balance is represented by

$$\dot{Q}_{evap} = \dot{m}_r(h_1 - h_4) = \dot{m}_r U_{evap} A_{evap}\left(T_{evap} - T_{amb}\right), \quad (2)$$

with $\dot{m}_r$ the refrigerant mass flow rate, h_1 and h_4 specific enthalpies. On the air side T_{evap} is the average surface temperature, U_{evap} the overall heat transfer coefficient, and A_{evap} the surface area.

The evaporator model employed a Kriging-assisted three-zone model (Huang et al., 2020), which accounts for the existence of a two-phase and a superheated region. For the condenser, a constant effectiveness was arbitrarily assumed. Compressor parameters like rotation n, isentropic efficiency η_{iso}, displacement $Disp$, and volumetric efficiency η_{vol} are required to solve the model. Additionally, the gas entering the compressor is superheated, and the liquid exiting the condenser is subcooled. In the present study frost formation was not considered.

Thermal Energy Storage

In the referred system a water tank was incorporated to store sensible thermal energy operating as a buffer between the HP and the radiators distributing heat to the indoors. Pump B drives the water between the condenser and the TES. A second circuit is used to recirculate water between the tank and the *n* existing radiators. It is assumed the water in the tank is fully mixed (uniform temperature), hence $T_8 = T_6$ in every step of time. If a stratified tank model were to be adopted, the temperature in the bottom (T_8) would be significantly lower than the one at the tank top. As the heat pump COP decreases with the rise of T_8, the system performance would improve if a stratified tank model was employed, thus the results of the current study are conservative. In the present model the energy balance of the water tank can be written as

$$\rho V C_p \frac{dT_{tank}}{dt} = \dot{Q}_{in} - \dot{Q}_{out} - \dot{Q}_{loss} - \dot{Q}_{load}, \quad (3)$$

with V the tank volume m^3 (ft^3), ρ the water specific mass kg/m^3 (lb/ft^3), and C_p the water specific heat J/kg.K (Btu/lb.ºF), the last two evaluated at the water tank temperature. The term in the left-hand side represents the rate of energy change in the tank, while the energy entering is $\dot{Q}_{in}$ and exiting the tank is $\dot{Q}_{out}$, the convective heat loss to the environment is $\dot{Q}_{loss}$. They can be calculated by

$$\dot{Q}_{in} = \dot{m} C_{p,w} (T_5 - T_8), \quad (4)$$

$$\dot{Q}_{out} = \dot{m} C_{p,w} (T_7 - T_6), \quad (5)$$

$$\dot{Q}_{loss} = hA(T_8 - T_{indoor}). \quad (6)$$

Water enters and leaves the tank at the same mass flow rate of $\dot{m}$ in kg/s (lb/s). $C_{p,w}$ was evaluated at the tank temperature. The overall heat transfer coefficient between the water and the air surrounding the tank is represented by h in W/m^2 ºC (Btu/h.ft^2.ºF). The surface area A is given in m^2 (ft^2). The heat transfer between the thermal storage tank and the radiators was exactly the heating load, $\dot{Q}_{load}$ in Equation (3). Since the goal of the present study is to assess the effect of integrating TES into the ASHP, detailed modeling of radiators is neglected; hence, they were modeled as ideal heat exchangers.

Residential Heating Load

The thermal load was calculated for a detached single-family 120 m^2 (1,291.67 m^2) dwelling, following the residential load factor method from the ASHRAE Handbook (American Society of Heating, Refrigerating, 2016).

$$\dot{Q}_{load} = AU(T_{amb} - T_{indoor}), \quad (7)$$

where A is the surface area and U is the construction factor. Equation (7) is used to calculate the contribution of the walls (A_{wall} =132 m^2 (1,420.84 ft^2) / U_{wall} = 0.51 W/m^2 ºC (0.0898 Btu/h.ft^2.ºF)) and the ceiling (A_c = 120 m^2 (1,291.67 ft^2) / U_c = 0.18 W/m^2.ºC (0.0317 Btu/h.ft^2.ºF)) (ASHRAE, 2005). Considering our goal, we keep the thermal load model as simple as possible; hence, we do not consider the contribution of infiltration and internal loads.

Model Validation

To verify the model's capability of representing the operation of a real HP we compared our simulated results with experimental data of a 10,257 W (35000 Btu/h) Carrier heat pump unit evaluated in a controlled environment at the National Renewable Energy Laboratory by (Shoukas et al., 2022), as displayed in Figure 2. The indoor temperature was kept at 22ºC (72°F), while the air outdoor temperature was varied from -13ºC (9.7°F) to 18 ºC (64.5°F). We simulated the heat pump using the same input parameters so the predictions on the COP and the system heating capacity could be compared.

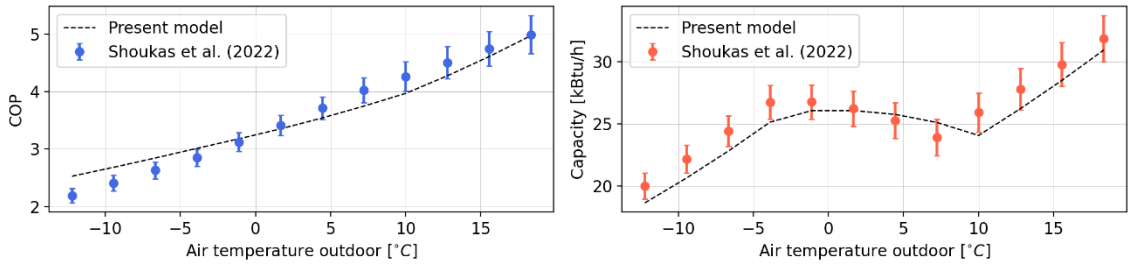

Figure 2 Model results compared to experimental data by (Shoukas et al., 2022).

For COP prediction the maximum relative deviation is 10% and for heat capacity 6.58%. The model predicted the trend over the entire outdoor air temperature range.

Metrics and Performance

Rating the performance of TES integrated with ASHP is challenging (Kaur et al., 2020), and different strategies have been adopted. In the present study we evaluated the system COP, seasonal performance factor (SPF), energy consumed, operational cost, and equivalent CO_2 emission. The COP is defined by Moran et al. (2006) as

$$COP(t) = \frac{\dot{Q}_{cond}(t)}{\dot{W}_{comp}(t)} \quad (8)$$

with $\dot{Q}_{cond}$ the rate of heat released by the condenser, and $\dot{W}_{comp}$ the power used by the compressor, both in W (Btu/h). This metric relates only the operation performance of the HP, which is significantly affected by the outdoor temperature and the temperature of the fluid entering the condenser, T_8. To account for the operation of the whole system over time, the SPF was calculated by

$$SPF = \frac{\sum_{t=0}^{8760} \dot{Q}_{load}(t)}{\sum_{t=0}^{8760} \dot{W}_{comp}(t)}. \quad (9)$$

This metric uses the annual heating load and annual work performed by the compressor to rate the system performance in the analyzed period (Masip et al., 2019). The costs of operation were calculated considering the electricity consumed and the respective electricity rate,

$$C_{ope} = \sum_{t=0}^{8760} \dot{W}_{comp}(t) El_r. \quad (10)$$

The electricity rate may vary depending on the location, and the model allows for simulating electricity rates varying as a function of the hour in the year. The last metric analyzed was the equivalent CO_2 emission, given by

$$CO_{2_{emt}} = \sum_{t=0}^{8760} \dot{W}_{comp} CO_{2_r}, \quad (11)$$

where the hourly energy spent by the system, W_{comp}, is multiplied by the carbon dioxide emission factor CO_{2_r} $kgCO_2/kWh$ ($lbCO_2/Btu$). This factor will change depending on the composition of the energy mix, i.e., locations with higher shares of renewables will present lower factors. Therefore, we simulated different scenarios to represent the system performance as a function of the energy mix composition.

Solution Scheme

Dynamic simulations are required to simulate the performance of the ASHP with the TES, as the knowledge of the

previous state of charge (SOC) is necessary for each timestep and the solution is treated as a quasi-steady state within the timestep. Explicit time dependance scheme is adopted, and since the climate data is available in an hourly basis and the water tank is considered perfectly mixed, the system is solved with a timestep of 1 hour.

The enthalpy marching solution procedure (Winkler et al., 2008) was adopted to solve the cycle. First, the pressures in the compressor inlet (P_1) and outlet (P_2) are guessed, followed by calculations for all the states. After marching the cycle, the resultant P_1 and P_2 are compared with the initial guesses in an iterative scheme until the convergence criterion (10^{-6}) is achieved. Equations (3) to (7) were solved for each timestep, and the fluid properties were evaluated at the tank temperature of the last iteration, $T_{tank,[t-1]}$.

CASE STUDY

To illustrate the functionality of the model, we present a case study where the system operation was simulated for the year 2021 in Denver, CO, using climate data from (Hersbach et al., 2018). Table 1 shows the adopted system parameters.

Table 1 – Parameters adopted to simulate the case study of Denver, CO - 2021.

Device	Parameter	Value
Heat pump	Subcooling	6.5 K (11.7 ºF)
	Superheating	8.5 K (15.3 ºF)
	Compressor – n	3600 rpm
	Compressor – $Disp$	5.37 x 10^{-5} m^3 (1.9 x 10^{-3} ft^3)
	Compressor – η_{iso}	0.63
	Compressor – η_{vol}	0.95
Condenser	HX effectiveness	0.7
Water tank	Radius	0.5 m (1.64 ft)
	Height	1.5 m (4.92 ft)
	h	1 W/m^2K (0.35 Btu/h.ft^2.ºF)
Pump B	$\dot{m}$	0.1 kg/s (0.22 l/s)

The overall heat transfer coefficient between the water and the air surrounding the tank was assumed to be h = 0.5 W/m^2 ºC (BTU/h.ft^2.ºF) (Le et al., 2020), for a tank with volume of 1.17 m^3 (41.32 ft^3). The refrigerant entering the compressor is superheated by 8.5 ºC, and the liquid exiting the condenser is subcooled by 6.5 ºC.

System Operation Logic

Several operation strategies can be adopted for an ASHP-TES hybrid system, and the system performance depends on the adopted strategy (Tarragona et al., 2020). Four different operation modes are defined, as displayed in Figure 3, and the operation mode at a given time is chosen according to the flowchart of Figure 4.

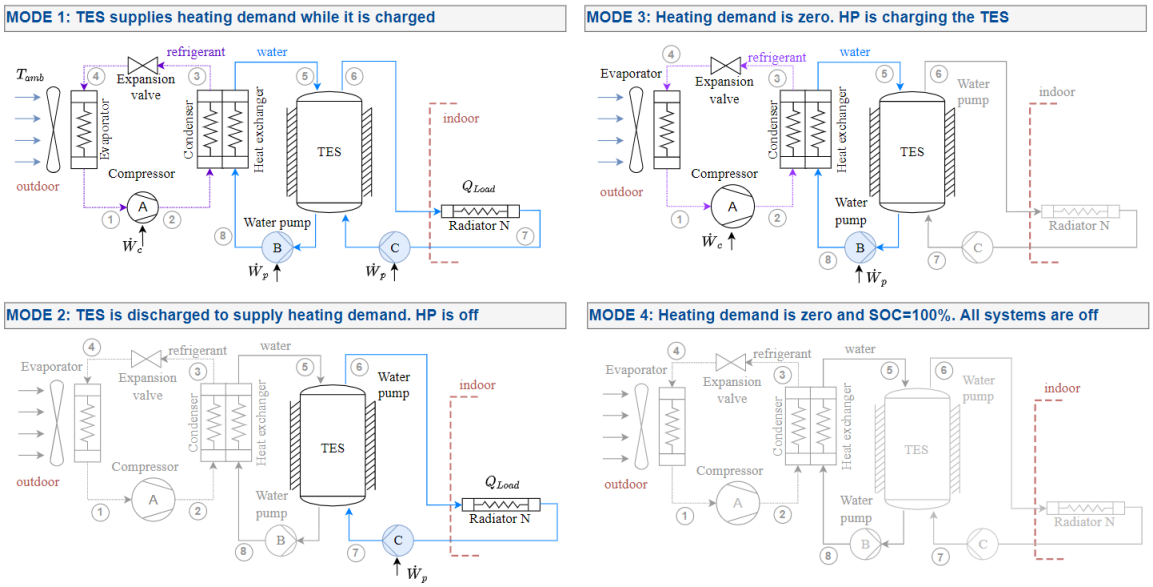

Figure 3 Operation modes. Circuits displayed in gray area not operating.

Several operation strategies can be adopted for an ASHP-TES hybrid system, and the system performance also depends on the adopted strategy (Tarragona et al., 2020). Figure 3 shows the operation logic proposed for the case studied. The system was designed so the TES is discharged whenever the outdoor temperature is lower than 7 ºC (44 ºF), to avoid operating the HP when the COP is lower. Because the water tank operates as a sensible TES, the SOC will vary with its temperature: 19ºC (66ºF) (SOC= 0%) to 72ºC (161ºF) (SOC= 100%). The indoor temperature setpoint is SP= 19ºC (66ºF).

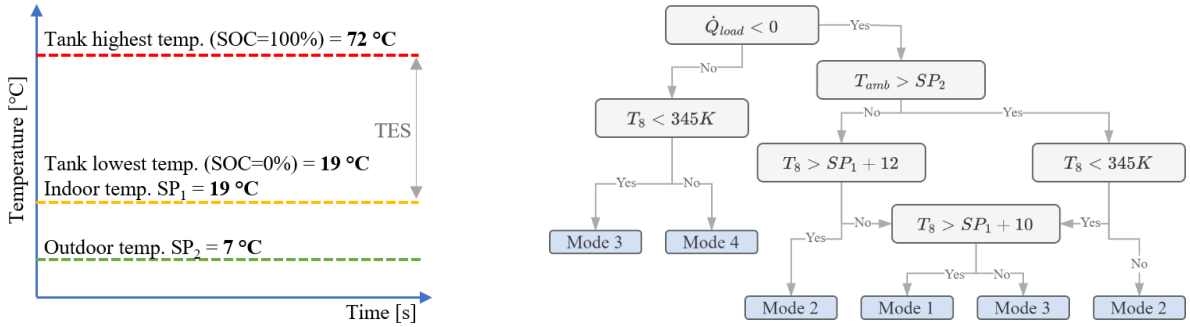

Figure 4 Logic adopted to control the system.

Four different operation modes were defined, as displayed in Figure 3, and the operation mode at a given time is chosen according to the flowchart of Figure 4. Additionally, it was arbitrarily defined that mode 2 can only be used if the SOC is higher than 18%, T_8 > SP+10ºC, guaranteeing the system will have enough energy to discharge the TES during the timestep period (3,600 s). In mode 4 even though all the systems are deactivated, the model keeps track of the heat losses from the TES to the environment.

Results

Annual results of temperature, heat transfer rates, and COP are presented in Figure 5. Since the system is only for heating, it does not operate between May and October (cooling season). The temperature of the refrigerant exiting the compressor (T_2) is the highest in the cycle and is only presented when the HP is on. T_5 is the temperature of the water leaving the condenser and follows the trend of T_2 given the constant effectiveness considered for the condenser. T_8 and T_6 are the temperature of the water in the tank. Since we defined that the TES is only discharged when T_{amb} < 7 ºC (44ºF), the tank temperature intentionally decreases during cold periods. The tank temperature also decreases because of tank losses $\dot{Q}_{loss}$ independently of the operation mode.

The thermal load $\dot{Q}_{load}$, the compressor work $\dot{W}_{comp}$, and the tank heat losses $\dot{Q}_{loss}$ are presented in the second plot of Figure 5. $\dot{Q}_{load}$ is calculated only when the outdoor temperature is below the setpoint of 19 ºC (66ºF). The compressor work changes with the saturation pressures in the condenser and evaporator because they affect the refrigerant specific mass, and consequently, the mass flow rate.

COP depends on the difference between the indoor and outdoor temperatures, and it was assumed that for a HP without TES (Figure 1b), the temperature of the water entering the condenser T_8 is constant SP + 20ºC (68ºF). For the ASHP-TES (Figure 1a), T_8 is the tank temperature, which can vary from 19 ºC (66ºF) (SOC=0%) to 72ºC (161ºF) (SOC=100%). The proposed logic prevents the heat pump of operating when the COP is low, hence, higher COP values were found when TES is included.

Albeit widely adopted, COP only represents an instantaneous picture of the system performance. The SPF, in turn, integrates the performance over time, including all the energy savings and losses. Hence, performance results integrated over one year are presented in Table 2. For the case studied, the SPF of the ASHP-TES system is almost 2% lower than the system without TES. The fact that the TES doesn't saved energy is related to the tank heat losses. In this study it is considered that the water tank is in a non-conditioned utility room. The overall performance of the system could be improved if the tank was placed, for instance, in the living room supplying the dwelling thermal load.

From an energy point of view, the studied ASHP-TES configuration is less efficient than the HP, therefore we explored the system performance regarding operation cost (electricity) and equivalent CO_2 emission. To evaluate a range of results, instead of adopting fixed values for the carbon dioxide emission factor (CO_{2_r}) and electricity rate (El_r), we simulated three scenarios presented in Figure 6. Scenario 1: lowest CO_{2_r}= 0.1 kgCO_2/kWh (6.4 x 10^{-5} lbCO_2/BTU),

representing high penetration of renewables (Masip et al., 2019), and the lowest electricity rate. Scenario 2: current average values for the United States (EIA, 2021), and scenario 3: highest historical electricity price and worst CO_{2_r}, representing an energy mix based on fossil fuels.

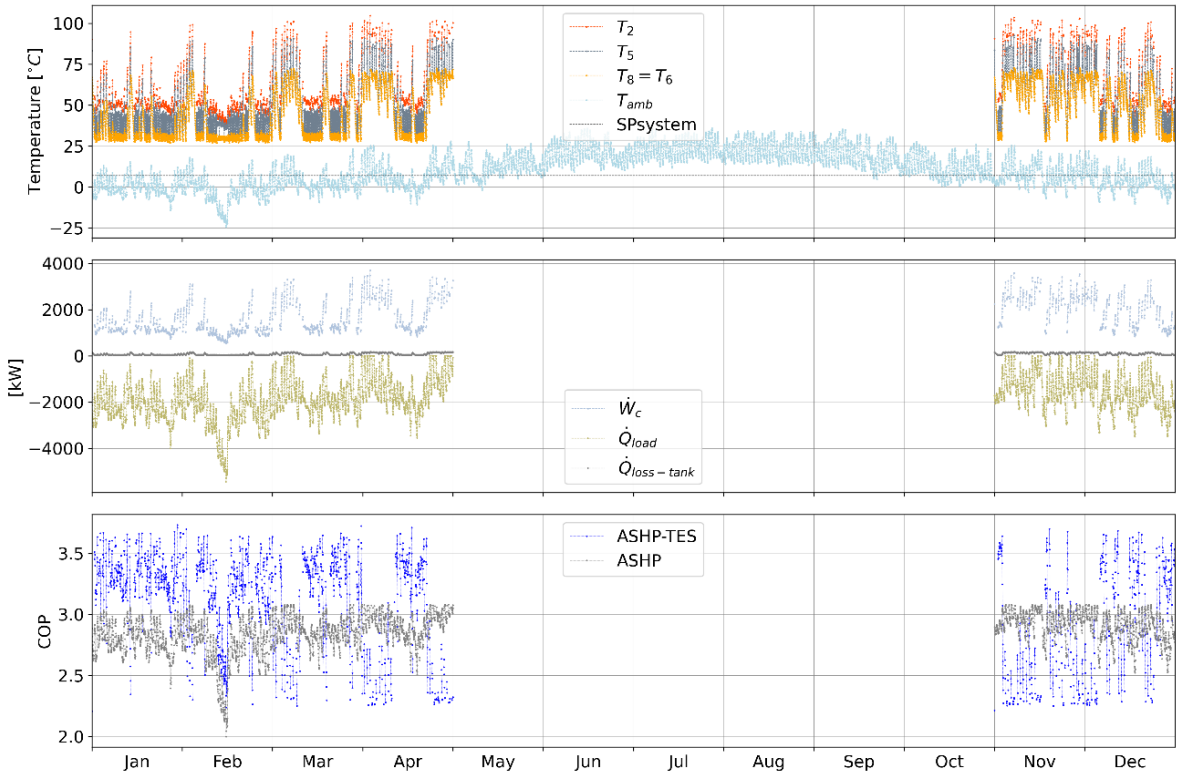

Figure 5 Temperatures, heat transfer rates, and COP for 8,760 h operation in Denver, CO.

Table 2 – Results for the standard heating system (without TES) and the ASHP-TES system.

Parameter	HP (no TES)	ASHP-TES
Average annual COP	2.85	3.09
SPF	2.91	2.85
Energy consumed [kWh]	3702	3754
Operation cost, C_{ope} [US$]	372	379
Carbon dioxide emission, $CO_{2_{emt}}$ [kg]	1054	1074
Energy saved with TES	-	-1.94%

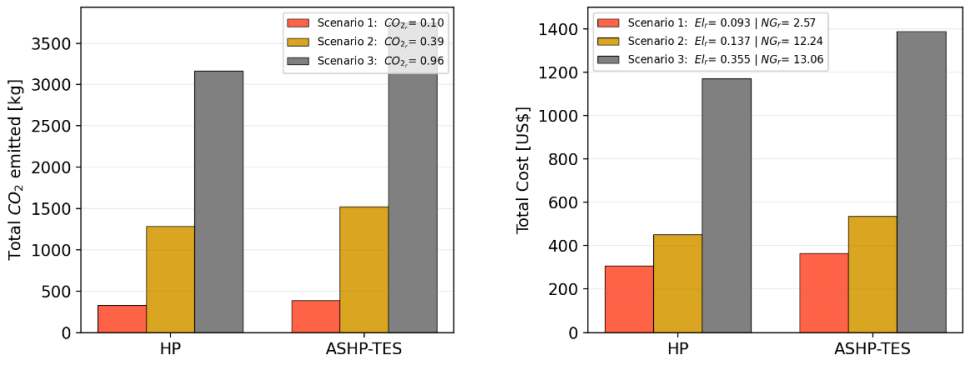

a b

Figure 6 Results for annual operation in Denver. (**a**) Total CO_2 emitted, (**b**) Total operation cost.

The results are highly influenced by the CO_2 factors and the electricity rates as observed in the ranges of Figure 6a and Figure 6b. In all scenarios the HP presents lower CO_2 emissions than the ASHP-TES solution, which follows the trend of the energy consumed by each system. As the ASHP-TES spends 1.94% more energy than ASHP, the CO_2 emission is also 1.94% higher. If we consider CO_2 emission rates changing in time, depending on the composition of the energy mix, the ASHP-TES could be used to shift the load to hours in which the production of renewables is higher.

Figure 6b shows that the total operation cost of the ASHP-TES was higher than the HP if a constant electricity rate is assumed. Yet, TES is expected to have its running cost reduced if time-of-use rates are introduced once it can shift the load to off-peak hours. In this example, no initial investment or maintenance costs were considered. If both electricity rates and CO_2 emission rates had their values changing in time, the decision on when to charge and discharge the TES would have to be oriented to minimize them instead of minimizing energy consumption.

CONCLUSIONS

In this study we expanded a previously developed Python framework to evaluate the effects of integrating thermal energy storage into air source heat pumps for space heating. The components are modeled separately as objects and the system solution considers the interaction between them in each timestep, using annual climate data for the desired location. A water tank is used as sensible TES operating in a buffer configuration between the HP and the radiators. Model validation is presented, using experimental data of a commercial heat pump tested in the National Renewable Energy Laboratory, and maximum relative deviations of 10% and 6.58% are found for the COP and heating capacity, respectively.

To illustrate how this model can be used to assess the ASHP-TES integration, a simulation example is provided. Climate data for Denver, Colorado feeds the model to assess the system operating over one year (2021). This example highlights some of the benefits and challenges of using a TES to prevent the HP of operating in very low temperatures. In the example, it is observed that no energy saving is accomplished by using TES. However, if TES is used to avoid peak load, the running costs would probably increase the system attractiveness. We observe that cost and environmental results are highly influenced by the characteristics of the local energy mix and the electricity costs.

If constant electricity and CO_2 emission rates are considered, the ASHP without TES presents better performance, since the storage device brings additional losses to the system. However, time-of-use rates for electricity and CO_2 emission may represent an opportunity to deploy ASHP-TES, as they could be used to shift the load to hours with high generation from renewables and lower costs. To justify the investment in additional equipment (TES) it is important to expand the metrics beyond the traditional ones like COP and SPF. Environmental and cost indicators are required to understand the role of ASHP-TES in a scenario towards decarbonization. The model will be further used to explore the relation between the adopted metrics and potential of using ASHP-TES in different regions of the United States.

ACKNOWLEDGMENTS

This study was financed in part by the *Coordenação de Aperfeiçoamento de Pessoal de Nível Superior – Brasil* (CAPES) – Finance Code 001. Conrado Ermel acknowledges *Conselho Nacional de Desenvolvimento Científico e Tecnológico* (CNPq) for his Ph.D. grant. Paulo S. Schneider acknowledges CNPq for his research grant (PQ301619/2019-0). This work was authored in part by the National Renewable Energy Laboratory, operated by Alliance for Sustainable Energy, LLC, for the U.S. Department of Energy (DOE) under Contract No. DE-AC36-08GO28308. Funding provided by the U.S. Department of Energy Office of Energy Efficiency and Renewable Energy Building Technologies Office. The views expressed in the article do not necessarily represent the views of the DOE or the U.S. Government. The U.S. Government retains and the publisher, by accepting the article for publication, acknowledges that the U.S. Government retains a nonexclusive, paid-up, irrevocable, worldwide license to publish or reproduce the published form of this work, or allow others to do so, for U.S. Government purposes.

NOMENCLATURE

A	=	area (m^2 | ft^2)
C_{op}	=	total heat pump operation cost (US$)
C_p	=	specific heat capacity (kJ/kg ºC | Btu/lb ºF)
$CO_{2_{emt}}$	=	total CO_2 emission (kg | lb)
CO_{2_r}	=	CO_2 emission factor ($kgCO_2/kWh$ | $lbCO_2/lbWh$)
$Disp$	=	compressor displacement (m^3 | ft^3)

El_r = electricity rate (US$/kWh | US$/Btu)
h, U = overall heat transfer coefficient (W/m^2 ºC | Btu/h.ft^2.ºF)
$\dot{m}$ = mass flow rate (kg/s | lb/s)
n = compressor rotation (rpm)
P = pressure (Pa | PSI)
$\dot{Q}$ = heat transfer rate (W | Btu/h)
Q = heat transfer (kWh | Btu)
T = temperature (ºC | ºF)
t = time (h)
V = volume (m^3 | ft^3)
$\dot{W}$ = work rate (W | Btu/h)
W = work (kWh | Btu)
ρ = specific mass (kg/m^3 | lb/ft^3)
η_{iso} = isentropic efficiency
η_{vol} = volumetric efficiency

Subscripts

c = ceiling
comp = compressor
Cond = condenser
eve = evaporator
in = inlet
loss = heat loss in the tank
load= residence heating load
out = outlet
w = water
wall= residence wall

REFERENCES

American Society of Heating, Refrigerating, and A.E., 2016. 2016 ASHRAE handbook HVAC systems and equipments (SI edition). Atlanta, GA, USA, USA.

ASHRAE, 2005. 2005 ASHRAE Handbook—Fundamentals (SI).

Bianco, V., Scarpa, F., Tagliafico, L.A., 2017. Estimation of primary energy savings by using heat pumps for heating purposes in the residential sector. Appl. Therm. Eng. 114, 938–947. https://doi.org/10.1016/j.applthermaleng.2016.12.058

Carroll, P., Chesser, M., Lyons, P., 2020. Air Source Heat Pumps field studies: A systematic literature review. Renew. Sustain. Energy Rev. 134. https://doi.org/10.1016/j.rser.2020.110275

da Cunha, J.P., Eames, P.C., 2016. Phase change materials to meet domestic space heating demand in the UK-A numerical study. Proc. World Congr. Mech. Chem. Mater. Eng. 1–8. https://doi.org/10.11159/htff16.145

Dincer, I., Rosen, M.A., Ahmadi, P., 2017. Optimization of energy systems, 1st ed. John Wiley and Sons Ltd.

EIA, 2021. How much carbon dioxide is produced per kilowatthour of U.S. electricity generation? [WWW Document]. US Energy Inf. Adm. URL https://www.eia.gov/tools/faqs/faq.php?id=74&t=11#:~:text=In 2020%2C total U.S. electricity,CO2 emissions per kWh. (accessed 3.15.22).

Ermel, C., Bianchi, M.V.A., Cardoso, A.P., Schneider, P.S., 2022a. Thermal storage integrated into air-source heat pumps to leverage building electrification: a systematic literature review. Appl. Therm. Eng. 215, 118975. https://doi.org/10.1016/j.applthermaleng.2022.118975

Ermel, C., Bianchi, M.V.A., Schneider, P.S., 2022b. Energy model of an air source heat pump to explore performance improvements under cold conditions: a Python™ framework, in: 7th International High Performance Buildings Conference at Purdue. Indiana.

Hersbach, H., Bell, B., Berrisford, P., Biavati, G., Horányi, A., Muñoz Sabater, J., Nicolas, J., Peubey, C., 2018. ERA5 hourly data on pressure levels from 1979 to present. [WWW Document]. Copernic. Clim. Change Serv. C3S Clim. Data Store CDS. https://doi.org/10.24381/cds.bd0915c6

Hirvonen, J., Sirén, K., 2017. High latitude solar heating using photovoltaic panels, air-source heat pumps and borehole thermal energy storage, in: Renne D. Griffiths S., R.M.G.K.M.D. (Ed.), ISES Solar World Congress 2017 - IEA SHC International Conference on Solar Heating and

Cooling for Buildings and Industry 2017, Proceedings. International Solar Energy Society, pp. 1907–1916. https://doi.org/10.18086/swc.2017.29.06

Huang, R., Ling, J., Aute, V., 2020. Comparison of approximation-assisted heat exchanger models for steady-state simulation of vapor compression system. Appl. Therm. Eng. 166, 114691. https://doi.org/10.1016/j.applthermaleng.2019.114691

IEA, 2022a. IEA – International Energy Agency [WWW Document]. Ctries. Reg. URL https://www.iea.org (accessed 12.1.22).

IEA, 2022b. A 10-point plan to reduce the european union' s reliance on russian natural gas. International Energy Agency.

Jiankai, D., Yiqiang, J., Shiming, D., Yang, Y., Minglu, Q., 2012. Improving reverse cycle defrosting performance of air source heat pumps using thermal storage-based refrigerant sub-cooling energy. Build. Serv. Eng. Res. - Technol. 33, 223–236. https://doi.org/10.1177/0143624411406016

Kaur, S., Bianchi, M., James, N., Berkeley, L., Kaur, S., Bianchi, M., James, N., 2020. 2019 Workshop on Fundamental Needs for Dynamic and Interactive Thermal Storage Solutions for Buildings 2019 Workshop on Fundamental Needs for Dynamic and Interactive Thermal Storage Solutions for Buildings.

Le, K.X., Huang, M.J., Shah, N.N., Wilson, C., Artain, P. Mac, Byrne, R., Hewitt, N.J., 2019. Techno-economic assessment of cascade air-to-water heat pump retrofitted into residential buildings using experimentally validated simulations. Appl. Energy 250, 633–652. https://doi.org/10.1016/j.apenergy.2019.05.041

Le, K.X., Huang, M.J., Wilson, C., Shah, N.N., Hewitt, N.J., 2020. Tariff-based load shifting for domestic cascade heat pump with enhanced system energy efficiency and reduced wind power curtailment. Appl. Energy 257, 113976. https://doi.org/10.1016/j.apenergy.2019.113976

Li, Y., Zhang, N., Ding, Z., 2020. Investigation on the energy performance of using air-source heat pump to charge PCM storage tank. J. Energy Storage 28. https://doi.org/10.1016/j.est.2020.101270

Long, Z., Jiankai, D., Yiqiang, J., Yang, Y., 2014. A novel defrosting method using heat energy dissipated by the compressor of an air source heat pump. Appl. Energy 133, 101–111. https://doi.org/10.1016/j.apenergy.2014.07.039

Masip, X., Cazorla-Marín, A., Montagud-Montalvá, C., Marchante, J., Barceló, F., Corberán, J.M., 2019. Energy and techno-economic assessment of the effect of the coupling between an air source heat pump and the storage tank for sanitary hot water production. Appl. Therm. Eng. 159. https://doi.org/10.1016/j.applthermaleng.2019.113853

Moran, M.J., Shapiro, H.N., Moran, M.J., 2006. Fundamentals of Engineering Thermodynamics, 1st ed. John Wiley & Sons Ltd, San Francisco.

Moreno, P., Sole, C., Castell, A., Cabeza, L.F., 2014. The use of phase change materials in domestic heat pump and air-conditioning systems for short term storage: A review. Renew. Sustain. Energy Rev. 39, 1–13. https://doi.org/10.1016/j.rser.2014.07.062

Sevault, A., Bohmer, F., Næss, E., Wang, L., 2019. Latent heat storage for centralized heating system in a ZEB living laboratory: Integration and design. IOP Conf. Ser. Earth Environ. Sci. 352. https://doi.org/10.1088/1755-1315/352/1/012042

Shoukas, G., Bonnema, E., Paranjothi, G., Faramarzi, R., Klun, L., Shoukas, G., Bonnema, E., Paranjothi, G., Faramarzi, R., Klun, L., 2022. Performance Assessment of High Efficiency Variable Speed Air-Source Heat Pump in Cold Climate Applications. NREL, Golden, CO.

Tarragona, J., Fernández, C., Cabeza, L.F., de Gracia, A., 2020. Economic evaluation of a hybrid heating system in different climate zones based on model predictive control. Energy Convers. Manag. 221, 113205. https://doi.org/10.1016/j.enconman.2020.113205

Treichel, C., Cruickshank, C.A., 2021. Economic analysis of heat pump water heaters coupled with air-based solar thermal collectors in canada and the united states. J. Build. Eng. 35, 102034. https://doi.org/10.1016/j.jobe.2020.102034

Vering, C., Maier, L., Breuer, K., Krützfeldt, H., Streblow, R., Müller, D., 2022. Evaluating heat pump system design methods towards a sustainable heat supply in residential buildings. Appl. Energy 308, 118204. https://doi.org/10.1016/j.apenergy.2021.118204

Wang, Z., Wang, F., Wang, X., Ma, Z., Wu, X., Song, M., 2017. Dynamic character investigation and optimization of a novel air-source heat pump system. Appl. Therm. Eng. 111, 122–133. https://doi.org/10.1016/j.applthermaleng.2016.09.076

Winkler, J., Aute, V., Radermacher, R., 2008. Comprehensive investigation of numerical methods in simulating a steady-state vapor compression system. Int. J. Refrig. 31, 930–942. https://doi.org/10.1016/j.ijrefrig.2007.08.008

Yu, M., Li, S., Zhang, X., Zhao, Y., 2021. Techno-economic analysis of air source heat pump combined with latent thermal energy storage applied for space heating in china. Appl. Therm. Eng. 185. https://doi.org/10.1016/j.applthermaleng.2020.116434